Construction and Characterization of a Heterodimeric Iron Protein: Defining Roles for Adenosine Triphosphate in Nitrogenase Catalysis†

Jeannine M. Chan,‡ Wei Wu,‡ Dennis R. Dean,*,§ and Lance C. Seefeldt*,‡

Department of Chemistry and Biochemistry, Utah State University, Logan, Utah 84322, and Department of Biochemistry−Fralin Biotechnology Center, Virginia Polytechnic University, Blacksburg, Virginia 24061

Received February 1, 2000; Revised Manuscript Received April 6, 2000

ABSTRACT: One molecule of MgATP binds to each subunit of the homodimeric Fe protein component of nitrogenase. Both MgATP molecules are hydrolyzed to MgADP and P_i in reactions coupled to the transfer of one electron into the MoFe protein component. As an approach to assess the contributions of individual ATP binding sites, a heterodimeric Fe protein was produced that has an Asn substituted for residue 39 in the ATP binding domain in one subunit, while the normal Asp^{39} residue within the other subunit remains unchanged. Separation of the heterodimeric Fe protein from a mixed population with homodimeric Fe proteins contained in crude extracts was accomplished by construction of a seven His tag on one subunit and a differential immobilized-metal-affinity chromatography technique. Three forms of the Fe protein (wild-type homodimeric Fe protein [Asp^{39}/Asp^{39}], altered homodimeric Fe protein [Asn^{39}/Asn^{39}], and heterodimeric Fe protein [Asp^{39}/Asn^{39}]) were compared on the basis of the biochemical and biophysical changes elicited by nucleotide binding. Among those features examined were the MgATP- and MgADP-induced protein conformational changes that are manifested by the susceptibility of the [4Fe-4S] cluster to chelation and by alterations in the electron paramagnetic resonance, circular dichroism, and midpoint potential of the [4Fe-4S] cluster. The results indicate that changes in the [4Fe-4S] cluster caused by nucleotide binding are the result of additive conformational changes contributed by the individual subunits. The [Asp^{39}/Asn^{39}] Fe protein did not support substrate reduction activity but did hydrolyze MgATP and showed MgATP-dependent primary electron transfer to the MoFe protein. These results support a model where each MgATP site contributes to the rate acceleration of primary electron transfer, but both MgATP sites must be functioning properly for substrate reduction. Like the altered homodimeric [Asn^{39}/Asn^{39}] Fe protein, the heterodimeric [Asp^{39}/Asn^{39}] Fe protein was found to form a high affinity complex with the MoFe protein, revealing that alteration on one subunit is sufficient to create a tight complex.

Molybdenum-dependent nitrogenase is composed of two component proteins called the MoFe protein and the Fe protein. The MoFe protein is a 240 kDa $\alpha_2\beta_2$ tetramer, with each $\alpha\beta$ dimeric unit containing one FeMo cofactor [Mo-8Fe-9*S*-homocitrate] and one [8Fe-7*S*] (P-cluster) (1). FeMo cofactor provides the site of substrate reduction (*2*), while the P-cluster is thought to provide an intermediate electron-transfer site between the Fe protein and FeMo cofactor (*3*−*6*). The Fe protein is a 64 kDa homodimer that has one nucleotide-binding site on each subunit and a single [4Fe-4S] cluster bridged between the two subunits (*7*). During catalysis, the Fe protein with two bound MgATP molecules associates with the MoFe protein. This association activates the hydrolysis of the two MgATP molecules, an event that is coupled to the transfer of a single electron from the Fe protein [4Fe-4S] cluster into the MoFe protein (*8*,*9*). The oxidized Fe protein, with two bound ADP molecules, then dissociates from the MoFe protein in a step that is believed to be rate-limiting for nitrogenase catalysis (*10*). This process is repeated until sufficient electrons have accumulated within the MoFe protein to permit substrate binding and reduction (*11*).

How MgATP binding and hydrolysis are coupled to intercomponent electron transfer and substrate reduction is a poorly defined aspect of the nitrogenase mechanism. The Fe protein is known to bind two nucleotides (either MgATP or MgADP) with the two binding events showing strong positive cooperativity (*12*). The binding of two MgADP or MgATP molecules induces protein conformational changes that have been detected as changes in the overall shape of the Fe protein (*13*) and as changes in the electronic and redox properties of the [4Fe-4S] cluster (*14*, *15*). These nucleotide-induced protein conformational changes are thought to have an important role in the nitrogenase mechanism.

One approach that has been used to probe the nitrogenase catalytic mechanism has involved placing amino acid substitutions within the nucleotide binding sites located within the Fe protein (*16*−*21*). One amino acid substitution in the homodimeric Fe protein that has proven informative is the substitution of residue Asp^{39} by Asn^{39} (*20*). Inspection of the crystallographic structure of the Fe protein (*7*) indicates that the carboxylate of Asp^{39} interacts with bound nucleotide

† Research supported by National Science Foundation Grants MCB-9722937 (to L.C.S.) and MCB-9630127 (to D.R.D.).

*Address correspondence to either author. L.C.S.: phone (435) 797-3964; fax (435) 797-3390; e-mail seefeldt@cc.usu.edu. D.R.D.: phone (540) 231-5895; fax (540) 231-7126; e-mail deandr@vt.edu.

‡ Utah State.

§ Virginia Tech.

10.1021/bi000219q CCC: $19.00
Published on Web 05/20/2000

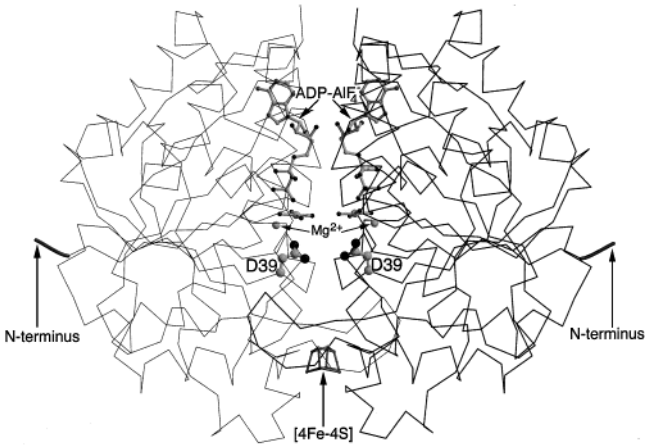

FIGURE 1: Structure of the Fe protein. The α-carbon trace of the Fe protein is depicted from the X-ray crystal structure (*47*) of the Fe protein complexed with the MoFe protein with bound MgADP−AlF_4^-, with one subunit presented as a thin line and the other as a thicker line. The positions of the bound Mg^{2+}, ADP−AlF_4^-, Asp^{39}, the N-terminus, and the [4Fe-4S] cluster are shown. The MoFe protein docking surface is at the bottom of the figure. The figure was generated with MOLSCRIPT (*48*) and Raster 3D (*49*).

through the Mg^{2+} cation and is part of a protein chain that connects the nucleotide binding site to the surface of the protein that associates with the MoFe protein (Figure 1). Substitution of Asp^{39} by Asn does not appear to significantly alter the binding of the nucleotides to the Fe protein, but it does alter the coupling of this binding to downstream events (*20*). For example, the MgATP- and MgADP-induced protein conformational changes elicited by nucleotide binding are impacted for the altered protein. In addition, the altered Fe protein shows only limited MgATP hydrolysis when combined with the MoFe protein, and no substrate reduction can be detected. The altered Fe protein is capable of very slow electron transfer to the MoFe protein, but following electron transfer, the altered Fe protein does not effectively dissociate from the MoFe protein. It was concluded that Asp^{39} participates in a nucleotide signal transduction pathway involved in component protein dissociation.

Because the Fe protein is a homodimer with each subunit coded for by the single *nifH* gene (*22*), any mutation results in production of an altered homodimeric Fe protein that carries an amino acid substitution on each subunit. In the present work, we have developed genetic and biochemical strategies for the production and purification of a heterodimeric Fe protein for which one subunit retains the normal Asp^{39} residue and the corresponding position in the other subunit is substituted by Asn^{39}. In this way it was possible to evaluate the contributions provided by each subunit of the Fe protein to events initiated and controlled by nucleotide binding and hydrolysis.

EXPERIMENTAL PROCEDURES

Strain Constructions. Strain DJ1274 was constructed in four steps (Figure 2). In the first step, the wild-type *Azotobacter vinelandii* was transformed with a recombinant plasmid (pDB1051) that contains a portion of the *nifH* gene and flanking genomic sequences, for which a small deletion was placed in the N-terminal coding sequence of *nifH* and

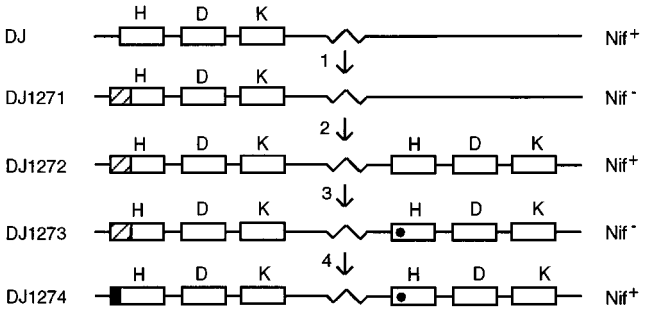

FIGURE 2: Schematic view of genetic constructs. The *nifH*, *nifD*, and *nifK* genes are indicated as boxes on each line. Strain DJ is the parental wild-type strain. The Nif phenotype is shown to the right of each strain designation. The deletion located within the N-terminal coding sequence of *nifH* in strains DJ1271, 1272, and 1273 is indicated as a hatched region. The polyhistidine coding sequence located at the N-terminal coding regions within DJ1274 is indicated as a solid region. The mutation leading to the Asn^{39} substitution in DJ1273 and DJ1274 is indicated as a solid dot. Steps 1−4 of the constructions are outlined in the Experimental Procedures section.

replaced with a Km^R [1] gene cartridge. In this way the deletion and insertion within pDB1051 was transferred to the *A. vinelandii* chromosome. Plasmids used in these constructions are not capable of autonomous replication in *A. vinelandii*.

In the second step, DJ1272 was constructed by transforming DJ1271 back to the Nif-plus phenotype with plasmid pDB196. Plasmid pDB196 contains the intact *nifHDK* gene cluster. Plasmid pDB196 also contains *nifF* coding sequences (flavodoxin) preceding the cloned portion of *nifH* and following the cloned portion of *nifK*. Thus, transformation of DJ1274 to the Nif-plus phenotype could occur either through homologous recombination within the *nifHDK* region, yielding the original wild-type genotype, or by homologous recombination with the *nifF* coding sequences. The *nifF* gene is located approximately 29 kilobases downstream from the *nifHDK* cluster, and *nifF* activity is not required for the Nif-plus phenotype. Homologous recombination of pDB196 with the *nifF* gene should lead to formation of a merodiploid strain that contains two copies of the *nifHDK* gene cluster. The correct construction of DJ1272 was confirmed by the retention of the original Km^R phenotype exhibited by DJ1271.

In the third step, strain DJ1272 was transformed to the Nif-minus phenotype by using plasmid pDBLCS792 as the donor DNA to yield DJ1273. Plasmid pDBLCS792 carried a *nifH* gene for which the Asp^{39} codon had been substituted by an asparagine codon (*20*). Because this strain still exhibits the original Km^R phenotype it can be concluded that both copies of the *nifHDK* gene clusters have been retained in DJ1273. In the final step strain DJ1274 was constructed by transforming DJ1273 to the Nif-plus phenotype by using

[1] Abbreviations: homodimeric [Asp^{39}/Asp^{39}] Fe protein, wild-type iron protein with aspartic acid at position 39 on both subunits; homodimeric [Asn^{39}/Asn^{39}] iron protein, iron protein with asparagine at position 39 on both subunits; heterodimeric [Asp^{39}/Asn^{39}] Fe protein, iron protein with one subunit containing aspartic acid at position 39 and the other subunit containing asparagine at position 39; EPR, electron paramagnetic resonance; MOPS, 3-(*N*-morpholino)propanesulfonic acid; Tris, tris(hydroxymethyl)aminomethane; HEPES, 4-(2-hydroxyethyl)-1-piperazineethanesulfonic acid; Km^R, kanamycin resistant; Km^S, kanamycin sensitive; Nif-plus, nitrogen fixation plus; Nif-minus, nitrogen fixation minus.

plasmid pDB1002 as the donor. This plasmid contains the *nifH* gene for which cassette mutagenesis was used to insert seven tandem histidine codons at the N-terminus of *nifH*. Strain DJ1274 retains two copies of the *nifHDK* gene cluster and should express both a His-tagged wild-type Fe protein subunit and a nontagged Fe protein subunit having the Asp^{39} residue substituted by asparagine.

Strain DJ1298 was constructed by transforming DJ1272 to the Km^S phenotype by using plasmid pDB1002 as the donor DNA. Strain DJ1298 retains two copies of the *nifHDK* gene cluster and should express both a His-tagged wild-type Fe protein subunit and a nontagged wild-type Fe protein subunit.

Protein Expression and Purification. Wild-type Fe and MoFe proteins were expressed in *A. vinelandii* cells and purified as previously described (*17*, *23*) with specific activities >1800 nmol of C_2H_2 reduced^{-1} min^{-1} mg. Fe proteins were expressed from the appropriate strain by the urea/N_2 derepression protocol (*17*). Fe proteins were purified to apparent homogeneity by a combination of ion-exchange and gel filtration chromatography as described (*17*). His-tagged Fe proteins were further purified by a Zn-affinity chromatography system (*24*), with step gradient elution with buffer containing either 75 or 250 mM imidazole. Protein concentrations were determined by a modified biuret method with bovine serum albumin as the standard (*25*). Fe protein concentrations were also determined from the visible absorption spectrum, with an absorption coefficient for the oxidized protein of 13.3 mM^{-1} cm^{-1} at 400 nm (*26*). All manipulations of proteins were conducted in the absence of oxygen in sealed serum vials under an argon atmosphere or inside an anaerobic glovebox (Vacuum Atmospheres, Hawthorne, CA) with an argon gas atmosphere.

Protein Characterization. SDS−PAGE was done as previously described (*27*) with Coomassie blue staining. The molecular mass of each Fe protein subunit was determined by matrix-assisted laser desorption ionization time-of-flight mass spectrometry at the Biotechnology Core Facility of Utah State University. A 1 μL portion of protein solution (diluted in water with 0.1% trifluoroacetic acid) was mixed with 1.5 μL of matrix solution (a saturated solution of α-cyano-4-hydroxycinnamic acid in a 40% acetonitrile/0.1% trifluoroacetic acid solution in water) and allowed to dry on a target. Analysis was done with a TofSpec mass spectrometer (Micromass, Inc., Beverly, MA) with ionization by a nitrogen laser. The spectrometer was run in the linear mode with 20 kV acceleration voltage and in the positive ion mode. Both internal and external calibration was used to establish the mass range, with cytochrome *c* as the standard. N-Terminal amino acid sequences were determined at the Protein and Nucleic Acid Shared Facility at the Medical College of Wisconsin, Milwaukee.

Activities. Proton and acetylene reduction activities were determined as previously described at 30 °C with a MgATP regenerating system (*28*). MgATP hydrolysis rates were quantified following separation of ATP and ADP by high-performance liquid chromatography (HPLC) with a Supelcosil LC-18 column (4.6 mm × 25 cm; Supelco, Bellefonte, PA), a mobile phase of 100 mM KH_2PO_4 buffer, pH 6.0, containing 14% (v/v) methanol and 4 mM tetrabutylammonium hydrogen sulfate, and flow rates of 1.3−2.0 mL min^{-1} (*29*). Nucleotides were detected with a continuous flow UV−visible detector and a molar absorption coefficient of 15.4 mM^{-1} cm^{-1} at 259 nm for MgADP (*30*).

The ability of altered, inactive Fe proteins to bind to the MoFe protein was tested by a competition assay described earlier (*21*). Increasing quantities of the altered Fe protein (from 0 to 256 μg) were added to fixed concentrations of wild-type Fe protein (128 μg or 2 nmol) and MoFe protein (256 μg or 1 nmol). The percent of acetylene reduction activity remaining was plotted versus the ratio of altered Fe protein to wild-type Fe protein, and the data were fit to the Hill equation:

$$\text{percentage activity} = V_{max} - (V_{max}[S]^n)/(K_m + [S]^n) \quad (1)$$

where V_{max} is 100%, [S] is the concentration of active Fe protein, K_m is the Michaelis constant, and n is the cooperativity factor.

Spectroscopic Methods. X-band (9.64 GHz) EPR spectra were recorded on a Bruker ESP300E spectrometer equipped with a dual mode cavity and an Oxford ESR 900 liquid helium cryostat. All other parameters are noted in the figure legends.

Potentiometric redox titrations were performed essentially as previously described (*19*). Circular dichroism spectra were done on the indigo disulfonate oxidized Fe proteins essentially as previously described (*31*).

Fe Chelation. The chelation of iron from Fe proteins was followed spectrophotometrically by the formation of the Fe^{2+}−bathophenanthroline disulfonate (BPS) complex, which was taken to have an absorption coefficient of 22.14 mM^{-1} cm^{-1} at 534 nm (*32*). The Fe chelation assays were performed in 2 mL volume cuvettes with a 1-cm path length and fitted with serum stoppers. To each cuvette, 950 μL of a solution containing 1.0 mM BPS in 50 mM Tris buffer, pH 8.0, was added and deoxygenated by bubbling with argon for 6 min. Dithionite was added to a final concentration of 2 mM followed by the addition of Fe protein (4 mg or 0.06 μmol). The reactions were initiated by the addition of ATP and $MgCl_2$ to final concentrations of 1 and 2 mM, respectively.

Stopped-Flow Spectroscopy. Pre-steady-state absorbance changes resulting from the oxidation of the [4Fe-4S] cluster of the Fe protein were monitored with a Hi-Tech SF61 stopped-flow spectrophotometer equipped with data acquisition and curve-fitting software (Salibury, Wiltshire, U.K.). The SHU-61 sample-handling unit was kept inside an anaerobic chamber with a gas atmosphere of 95% N_2 and 5% H_2 with less than 1 ppm oxygen. Reactants were maintained at 23.0 ± 0.5 °C by means of a Techne C-85D circulator (Techne Ltd., Duxford, Cambridge, U.K.) attached to a FC-200 flow cooler (*33*). Data were collected at 430 nm. The reaction was initiated by rapid mixing of a solution containing 80 μM Fe protein and 10 mM dithionite in 50 mM HEPES buffer, pH 7.4, with a solution containing 20 μM MoFe protein, 10 mM dithionite, and 5 mM MgATP in 50 mM HEPES buffer, pH 7.4. The $[4Fe\text{-}4S]^{2+}$ cluster is protected from reduction by dithionite while the Fe protein is complexed to the MoFe protein. Therefore, the pre-steady-state increase in absorbance reflects the oxidation of the Fe protein [4Fe-4S] cluster upon primary electron transfer to the MoFe protein.

RESULTS

Construction and Purification of a Heterodimeric Fe Protein. The construction of a merodiploid strain of *A. vinelandii* containing two copies of the nitrogenase structural genes (*nifH*, *nifD*, and *nifK*) in the chromosome is outlined in Figure 2. The final strain (DJ1274) contains one copy of the Fe protein encoding gene (*nifH*) with an additional 21 nucleotides encoding seven His residues (His tag) on the N-terminus of the Fe protein subunit. The other copy of *nifH* contains an altered codon that results in the substitution of Asn for Asp at position 39. Expression of both copies of the *nifH* gene is directed from identical *nifH* promoter sequences located upstream of each gene copy. This promoter is activated upon removal of a fixed nitrogen source (e.g., conversion to diazotrophic growth), resulting in the expression of both sets of *nifHDK* genes. Assuming equal expression from both copies of the *nifH* gene and random assembly of the dimeric Fe protein, a mixed population of homodimeric and heterodimeric Fe proteins should accumulate. These include a wild-type homodimeric [Asp^{39}/Asp^{39}] Fe protein, an altered homodimeric [Asn^{39}/Asn^{39}] Fe protein, and a heterodimeric [Asp^{39}/Asn^{39}] Fe protein. The homodimeric [Asp^{39}/Asp^{39}] Fe protein carries a His tag on the N-terminus of both subunits, whereas the heterodimeric [Asp^{39}/Asn^{39}] Fe protein contains a His tag on only one of the subunits. The altered homodimeric [Asn^{39}/Asn^{39}] Fe protein does not contain a His tag on either subunit. The presence or absence of His tags located on the various Fe protein types present in a mixed population was used to specifically purify the heterodimeric [Asp^{39}/Asn^{39}] Fe protein as described below.

Fe proteins were first collectively purified from crude extracts of strain DJ1274 using traditional ion-exchange and gel-filtration chromatography (*17*). The purified proteins were then applied to a Zn-affinity column. A first fraction of the loaded Fe protein eluted from the column upon washing with buffer containing no imidazole. This protein was shown to be the altered homodimeric [Asn^{39}/Asn^{39}] Fe protein for which neither subunit carries a His tag. A second fraction of Fe protein was eluted from the column when washed with a buffer containing 75 mM imidazole. This protein was shown to be the heterodimeric [Asp^{39}/Asn^{39}] Fe protein that carries a His tag on only one of the subunits. A third fraction of Fe protein was subsequently eluted from the column by washing with buffer containing 250 mM imidazole. This protein was shown to be the wild-type homodimeric [Asp^{39}/Asp^{39}] Fe protein that contains a His tag on both subunits. A diploid strain (DJ1298) that produces a mixed population of His-tagged Fe proteins that do not have any amino acid substitutions was also constructed. By using strain DJ1298 and the purification strategy described above it was possible to isolate a homodimeric [Asp^{39}/Asp^{39}] Fe protein for which only one of the subunits carries a His tag. This homodimeric [Asp^{39}/Asp^{39}] Fe protein with a single His tag was used for control experiments.

The identity of the various Fe proteins used in the present work was confirmed by SDS−PAGE, mass spectrometry, and N-terminal protein sequence analysis. SDS−PAGE analysis of the heterodimeric Fe proteins revealed two protein bands on the SDS gel. The slower-migrating band (predicted to be a subunit with a His tag) migrated identically with the one band observed for the homodimeric [Asp^{39}/Asp^{39}] Fe protein for which both subunits carry a His tag. The faster-migrating band (predicted to be a subunit without a His tag) migrated identically with wild-type Fe protein and homodimeric [Asn^{39}/Asn^{39}] Fe proteins, neither of which carries a His tag on either subunit (data not shown).

Table 1: N-terminal Amino Acid Sequences and Mass Spectral Data for Fe Proteins

Fe protein source	subunit mass (Da)		N-terminal sequence
	sequence[a]	mass spectrometry	
[Asp^{39}/Asp^{39}][b]	31 365	31 317	AMRQCAIYGKGG[a]
[Asp^{39}/Asp^{39}][c]	32 587	32 565	MHHHHHHHMAMR
[Asp^{39}/Asn^{39}][d]	31 365	31 413	AMRQX[e]AIYGKGG
	32 587	32 547	MHHHHHHHMAMR

[a] Sequence predicted from the DNA sequence of the *nifH* gene (*22*). [b] Fe protein produced by the wild-type strain. Does not carry a His tag on either subunit. [c] Third Fe protein fraction eluted by the immobilized metal affinity chromatography technique. This protein is predicted to have an N-terminal His tag on both subunits. [d] Second Fe protein fraction eluted by the immobilized metal affinity chromatography technique. This protein is predicted to have one subunit that carries a His tag and one subunit that does not contain a His tag. [e] No single amino acid was detected at this position.

Table 2: Activities of Fe Proteins

Fe protein subunit composition	specific acitivity [nmol of product·min^{-1}·(mg Fe protein)$^{-1}$]			ATP/e^-
	C_2H_4	H_2	MgADP	
[Asp^{39}/Asp^{39}][a]	1810 ± 20	1960 ± 40	4640 ± 580	2.6 ± 0.4
[Asp^{39}/Asp^{39}][b]	1470 ± 20	1460 ± 60	3320 ± 230	3.2 ± 0.5
[Asn^{39}/Asn^{39}][c]	ND[e]	ND	14.0 ± 0.3	
[Asp^{39}/Asn^{39}][d]	ND	ND	280 ± 20	

[a] Fe protein produced by the wild-type strain. Does not contain a His tag on either subunit. [b] Fe protein purified from strain DJ1298. One subunit contains an N-terminal His tag, and the other subunit does not contain a His tag. [c] Homodimeric [Asn^{39}/Asn^{39}] Fe protein. Does not contain a His tag on either subunit. [d] Fe protein purified from DJ1274. One subunit contains an N-terminal His tag and the other subunit does not contain a His tag. [e] Not detected.

The molecular mass of the subunits of the various Fe proteins was determined by mass spectrometry, and the results are shown in Table 1. These results are all in line with predictions based on the known primary sequences of the individual subunits for each construct (*22*). The heterodimeric Fe protein showed two parent peaks in the mass spectrum, each with nearly identical intensity. One of these peaks shows a mass consistent with the presence of a His tag, whereas the other peak corresponds to the mass of a subunit that does not carry a His tag (Table 1). Finally, the N-terminal sequence was determined for the heterodimeric [Asp^{39}/Asn^{39}] Fe protein and compared to the N-terminal sequences of the wild-type Fe protein and an Fe protein that carries a His tag on both subunits of an otherwise wild-type protein (Table 1).

Characterization of His-Tagged Fe Proteins That Do Not Carry Amino Acid Substitutions. It was first necessary to determine the effect of N-terminal His tags on Fe protein catalytic function. Fe proteins carrying a His tag on either one or both of the subunits, but no other alterations within the Fe protein coding sequence, were observed to support high rates of proton and acetylene reduction activity (Table 2). MgATP hydrolysis rates were also similar to those supported by the nontagged Fe protein, and ATP/e^- ratios were nearly identical to those of nontagged Fe protein. The

Fe protein to MoFe protein ratio required for optimal activity was similar for all Fe proteins examined. In addition, the nucleotide induced conformational changes observed for His-tagged Fe proteins that are otherwise unaltered were identical to those of the nontagged wild-type Fe protein as assessed by EPR, CD, midpoint potential determinations, Fe chelation rates, and primary electron-transfer rates (described below). These results demonstrate that the presence of an N-terminal His tag on one or both subunits of the Fe protein does not prevent its proper functioning in catalysis. Wild-type Fe protein in the following sections refers to Fe protein with either one or two His tags.

Activities of the Heterodimeric [Asp^{39}/Asn^{39}] Fe Protein. Fe protein that has the Asp^{39} residue position substituted by Asn^{39} within both subunits showed no substrate reduction activity and only trace MgATP hydrolysis activity as reported earlier (*20*; Table 2). Similarly, the heterodimeric [Asp^{39}/Asn^{39}] Fe protein did not exhibit detectable substrate reduction activities, although this altered Fe protein did show MgATP hydrolysis activity that was approximately 5% of the wild-type rate only in the presence of the MoFe protein.

Nucleotide Interactions with the Heterodimeric Fe Protein. The wild-type Fe protein is known to bind two molecules of MgATP or MgADP (*7*), with the binding of either nucleotide resulting in characteristic changes in the line shape of the EPR spectrum of the [4Fe-4S]$^{1+}$ cluster (*14*, *34*, *35*), the visible region CD spectrum (*15*, *31*), the chelation rate of Fe from the cluster (*32*, *36*), and the E_m for the [4Fe-4S]$^{2+/1+}$ cluster couple (*14*). Monitoring of these features was then used to assess changes in the coupling of nucleotide binding to protein conformational changes within the heterodimeric [Asp^{39}/Asn^{39}] Fe protein.

All of the Fe proteins studied in the present work showed identical resting-state, rhombic EPR spectra in the absence of nucleotides, confirming that substitution of Asp^{39} within one or both Fe protein subunits does not alter the resting state of the [4Fe-4S] cluster (data not shown). Addition of MgATP to the wild-type Fe protein (or to His-tagged versions of the wild-type Fe protein) results in a line shape change to an axial signal ($g = 2.03$ and 1.92) (Figure 3). In contrast, an altered homodimeric [Asn^{39}/Asn^{39}] Fe protein shows little change in EPR spectrum upon addition of MgATP ($g = 2.06$, 1.94, and 1.86), indicating that the amino acid change has prevented MgATP-coupled changes to the electronic properties of the [4Fe-4S] cluster. Addition of MgATP to the heterodimeric [Asp^{39}/Asn^{39}] Fe protein was observed to result in an EPR spectrum with $g = 2.04$, 1.93, and a poorly defined third g-value. This line shape change appeared to be between the MgATP-bound wild-type Fe protein spectrum and the MgATP-bound form of the altered homodimeric [Asn^{39}/Asn^{39}] Fe protein spectrum as indicated by comparison to the additive spectrum of the wild-type Fe protein and the [Asn^{39}/Asn^{39}] Fe protein. This suggests a partial conformational change resulting from MgATP binding to the heterodimeric Fe protein.

The visible region CD spectrum of the oxidized Fe protein reports conformational changes around the oxidized [4Fe-4S] cluster upon binding nucleotides. Earlier studies showed that the Fe protein alone, the Fe protein with bound MgATP, and the Fe protein with bound MgADP each exhibits a unique CD spectrum (*31*). Substituting Asp^{39} by Asn^{39} within both Fe protein subunits was previously found to not alter either the nucleotide-free or the MgATP-bound CD spectrum when compared to wild-type Fe protein (20). However, transition to the MgADP-bound spectrum was prevented in the case of the homodimeric [Asn^{39}/Asn^{39}] form of the Fe protein. The heterodimeric [Asp^{39}/Asn^{39}] Fe protein also exhibited normal nucleotide-free and MgATP-bound spectra, indicating that substituting Asp^{39} to Asn^{39} for only one subunit does not perturb either the resting state of the protein or the MgATP-induced structural changes (data not shown). However, the spectrum for the MgADP-bound form of the heterodimeric [Asp^{39}/Asn^{39}] Fe protein was similar to the additive spectrum of the wild-type Fe protein and the homodimeric [Asn^{39}/Asn^{39}] Fe protein spectra in their MgADP-bound forms, suggesting partial ADP-induced conformational changes (Figure 4).

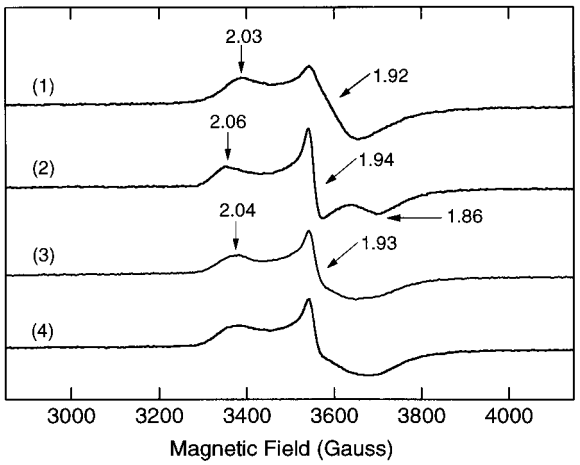

FIGURE 3: EPR spectra of Fe proteins in the presence of MgATP. Perpendicular mode EPR spectra for the wild-type homodimeric [Asp^{39}/Asp^{39}] Fe protein for which one subunit carries a His tag (trace 1), the homodimeric [Asn^{39}/Asn^{39}] Fe protein (trace 2), and the heterodimeric [Asp^{39}/Asn^{39}] Fe protein for which one subunit carries a His tag (trace 3). Trace 4 shows the additive spectrum of traces 1 and 2. Spectra were recorded at 12 K, with a microwave frequency of 9.64 GHz, a microwave power of 2 mW, a modulation frequency of 100 kHz, a modulation amplitude of 7.97 G, and a conversion time and time constant of 10.24 ms. Protein concentrations were 10 mg/mL in 100 mM Tris buffer, pH 8.0, with 2 mM dithionite and 1.6 mM MgATP.

A sensitive way to monitor MgATP-induced protein conformational changes within the Fe protein is the rate of chelation of Fe from the [4Fe-4S] cluster by chelators such as bathophenanthroline disulfonate (BPS) (*32*, *36*). Earlier studies revealed that addition of MgATP, but not MgADP, to the Fe protein substantially increased the rate of formation of Fe^{2+}-BPS, which can be monitored by an absorbance increase (*32*). The substitution of Asp^{39} by Asn^{39} in both subunits was found to greatly diminish the rate of Fe chelation upon addition of MgATP relative to the rate observed for the wild-type Fe protein (Figure 5). Substitution of Asp^{39} by Asn^{39} for only one Fe protein subunit resulted in a rate of Fe chelation that is between that observed for the wild-type Fe protein and the altered homodimeric [Asn^{39}/Asn^{39}] Fe protein. No Fe chelation was detected in the absence of MgATP for any of the Fe proteins.

The midpoint potential of the [4Fe-4S]$^{2+/1+}$ couple changes from -300 mV to -420 mV or -460 mV by the binding of MgATP or MgADP to the Fe protein, respectively (*14*, *19*). Substitution of Asp^{39} by Asn^{39} on both subunits of the

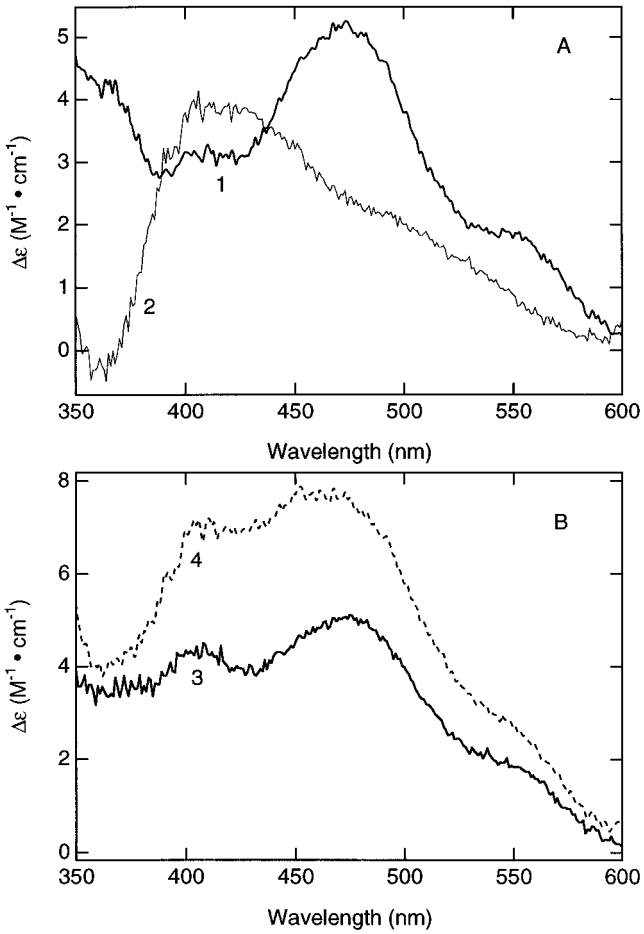

FIGURE 4: CD spectra of Fe proteins in the presence of MgADP. The visible region CD spectra of IDS-oxidized Fe proteins were recorded as described under Experimental Procedures. In panel A the CD spectra for a wild-type homodimeric [Asp^{39}/Asp^{39}] Fe protein for which both subunits carry a His tag (trace 1) and a homodimeric [Asn^{39}/Asn^{39}] Fe protein (trace 2) are shown. In panel B the spectrum of a heterodimeric [Asp^{39}/Asn^{39}] Fe protein for which one subunit carries a His tag (trace 3) is shown. Trace 4 shows the additive spectrum of traces 1 and 2. Protein concentrations were 100 μM in 100 mM Tris buffer, pH 8.0 with 1 mM ADP and 1.5 mM $MgCl_2$.

Fe protein did not change the E_m (−300 mV) in the absence of nucleotides from that observed for the wild-type Fe protein. However, the addition of MgADP to the altered homodimeric [Asn^{39}/Asn^{39}] Fe protein did not lower the E_m. Examination of the heterodimeric [Asp^{39}/Asn^{39}] Fe protein revealed that MgADP changes the E_m from −300 mV to −390 mV, intermediate between those changes elicited for the wild-type and homodimeric [Asn^{39}/Asn^{39}] Fe proteins (data not shown).

Interactions of a Heterodimeric Fe Protein with MoFe Protein. In the absence of MgATP, the Fe protein shows no detectable electron transfer to the MoFe protein. Upon the addition of MgATP, a primary electron-transfer event can be measured by stopped-flow spectrophotometry with an apparent first-order rate constant of ~100 s^{-1}. For the altered homodimeric [Asn^{39}/Asn^{39}] Fe protein, the MgATP-dependent primary electron transfer rate is greatly diminished, with an apparent first-order rate constant of 0.0025 s^{-1}. In contrast, the heterodimeric [Asp^{39}/Asn^{39}] Fe protein was observed to have a rate constant for primary electron transfer of 2.2 s^{-1}, which is between the rate constants observed for the wild-type and altered [Asn^{39}/Asn^{39}] homodimeric Fe proteins (Table 3). This observation indicates that each MgATP binding site contributes to the rate acceleration of primary electron transfer to the MoFe protein. While primary electron transfer was observed for all Fe proteins examined, the presence of Asn at position 39 in one or both subunits prevented reduction of substrates, which would require the delivery of at least two electrons into the MoFe protein.

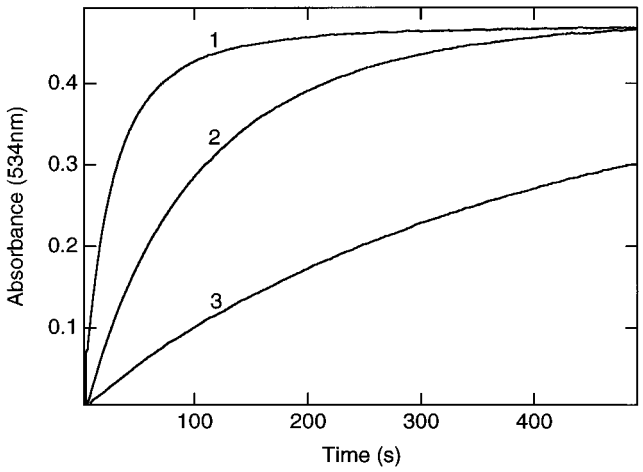

FIGURE 5: Time course for Fe chelation from Fe proteins. The time course for MgATP-dependent Fe chelation from Fe proteins was determined from the increase in absorbance at 534 nm from formation of Fe^{2+}-bathophenanthroline disulfonate (BPS) as described under Experimental Procedures. The Fe proteins used were a wild-type homodimeric [Asp^{39}/Asp^{39}] Fe protein for which one subunit carries a His tag (trace 1), a heterodimeric [Asp^{39}/Asn^{39}] Fe protein for which one subunit carries a His tag (trace 2), and a homodimeric [Asn^{39}/Asn^{39}] Fe protein (trace 3). Apparent first-order rate constants were 0.027, 0.009, and 0.003 s^{-1}, respectively.

Table 3: Primary Electron Transfer from Fe Proteins to MoFe Protein

Fe protein subunit composition	apparent first-order rate constant (s^{-1})
[Asp^{39}/Asp^{39}][a]	118 ± 15[b]
[Asp^{39}/Asp^{39}][c]	120 ± 10
[Asn^{39}/Asn^{39}][d]	0.025 ± 0.009
[Asp^{39}/Asn^{39}][e]	2.2 ± 1.0

[a] Fe protein produced by the wild-type strain. Does not contain a His tag on either subunit. [b] Standard deviations are from three independent measurements. [c] Fe protein purified from strain DJ1298. One subunit contains an N-terminal His tag, and the other subunit does not contain a His tag. [d] Altered Fe protein. Does not contain a His tag on either subunit. [e] Fe protein purified from DJ1274. One subunit contains an N-terminal His tag, and the other subunit does not contain a His tag.

Following primary electron transfer, the altered [Asn^{39}/Asn^{39}] homodimeric Fe protein forms an essentially non-dissociating complex with the MoFe protein. This situation contrasts with the wild-type Fe protein, where dissociation from the MoFe protein appears to occur following each electron-transfer event. Similar to the homodimeric [Asn^{39}/Asn^{39}] Fe protein, the heterodimeric [Asp^{39}/Asn^{39}] Fe protein forms a tight complex with the MoFe protein, as indicated by its ability to inhibit proper complex formation between the wild-type Fe protein with the MoFe protein (Figure 6).

DISCUSSION

Heterodimeric Fe Protein. A system has been developed that allows the expression and purification of heterodimeric

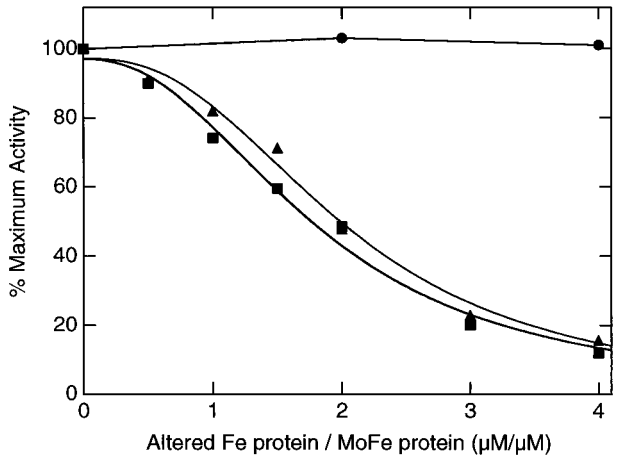

FIGURE 6: Inhibition of wild-type nitrogenase acetylene reduction activity by altered Fe proteins. Inhibition of wild-type nitrogenase acetylene reduction activity was performed as described under Experimental Procedures. Wild-type MoFe protein (256 μg, 1 nmol) was added to each assay vial. Different amounts (from 32 to 256 μg, or 0.5−4 nmol) of homodimeric [Asn^{39}/Asn^{39}] Fe protein (■), heterodimeric [Asp^{39}/Asn^{39}] Fe protein for which one subunit carries a His tag (▲), or bovine serum albumin (●) were added prior to initiation of the assay by the addition of 128 μg (2 nmol) of wild-type Fe protein. The percentage of the maximum activity observed in the absence of added inhibitor is plotted against the molar ratio of altered Fe protein to MoFe protein. The data were fit to the inverse Hill equation, where the cooperativity factor was found to be 2.5 for the heterodimeric [Asp^{39}/Asn^{39}] Fe and 2.3 for the homodimeric [Asn^{39}/Asn^{39}] Fe protein.

Fe proteins. There are two main elements to the approach developed here. First, expression and assembly of the heterodimer Fe protein occurs in vivo, allowing the proper maturation of the Fe protein. As is the case for many metalloproteins, the proper assembly of the mature protein involves accessory proteins. In this system, the Fe protein is expressed in *A. vinelandii*, where the appropriate genetic background is present to permit nitrogenase maturation. Because both copies of the *nifH* gene are expressed under the control of identical *nifH* promoters, expression from both genes is coordinate and balanced. The second element to the system is the presence of an N-terminal His tag on one of the two Fe protein subunits. This situation permits rapid and complete separation of homodimeric and heterodimeric Fe proteins from a mixed population of Fe proteins

During the design of the His-tagged constructs, examination of the X-ray structure of the Fe protein (*7*) suggested that placement of a His tag on either the C-terminus or the N-terminus would have minimal impact on the activities of the protein (Figure 1). However, placement of a His tag on the C-terminus of both subunits was found to significantly reduce the activity of the His tagged Fe protein, and so this construct was not pursued further. In contrast, addition of a His tag to the N-terminus of either one or both subunits of the Fe protein had minimal effect on activity or other properties of the Fe protein. Thus, these and other constructs derived from them were used in the current work.

ATP Interactions with Fe Protein. One of the open questions about the nitrogenase mechanism is how nucleotide binding and hydrolysis are coupled to conformational changes in the Fe protein. Extensive studies have been conducted to probe the protein conformational changes induced in the Fe protein upon binding nucleotides (*8,9*). Given the architecture of the Fe protein where nucleotides bind 15 Å away from the [4Fe-4S] cluster (*7*), protein conformational changes are the likely method for communication from the nucleotide binding site and the cluster (*16, 37*). In all previous studies, these conformational changes were examined with nucleotides interacting with both subunits of the Fe protein (*16*−*21, 37*−*44*). In the present study, with the heterodimeric Fe protein, it was possible to probe the contributions of nucleotide interactions from each subunit on the overall conformational changes imposed on the [4Fe-4S] cluster. The assessment of the nucleotide-induced protein conformations indicate that the heterodimeric [Asp^{39}/Asn^{39}] Fe protein undergoes conformational changes that are intermediate between those of the wild-type and altered homodimeric [Asn^{39}/Asn^{39}] Fe proteins. It therefore appears that the contributions to the protein conformational changes induced by each nucleotide binding are additive. This finding is supported by the earlier finding from titration calorimetry that suggested that the binding energy from two nucleotides is required to account for the change induced in the E_m of the cluster (*45*).

ATP Roles in the Fe Protein−*MoFe Protein Complex.* Results from the current work also address roles played by two nucleotides within the Fe protein−MoFe protein complex. Substitution of Asp^{39} by Asn^{39} within both subunits of the Fe protein lowers the MgATP-dependent primary electron rate by 4 orders of magnitude compared to that observed for the wild-type Fe protein. The heterodimeric [Asp^{39}/Asn^{39}] Fe protein was observed to have a primary electron-transfer rate 2 orders of magnitude higher than for the altered homodimeric [Asn^{39}/Asn^{39}] Fe protein but 2 orders of magnitude lower than for the wild-type Fe protein. This suggests that the proper functioning of one subunit of the Fe protein with regard to MgATP provides partial stimulation of the rate of electron transfer. The full acceleration of the rate of electron transfer would be predicted to result from the additive effects of the two MgATP binding/hydrolysis reactions. The order of MgATP hydrolysis and electron transfer has not been clearly defined (*46*), so in the present work the rate acceleration could result from either MgATP binding or hydrolysis.

Finally, the present results reveal that alteration on only one subunit of the Fe protein is sufficient to activate the formation of a tight complex between the Fe protein and the MoFe protein. Earlier it was found that the homodimeric [Asn^{39}/Asn^{39}] Fe protein formed a tight complex with the MoFe protein (*20*). In the present work, it is shown that the heterodimeric [Asp^{39}/Asn^{39}] Fe protein also forms a tight complex with the MoFe protein. Given that the docking interface on the MoFe protein is pseudosymmetric (*47*), it is possible that the heterodimeric Fe protein only forms a tight complex in a certain orientation with the MoFe protein.

In summary, we have developed a system for the production and isolation of a heterodimeric form of the nitrogenase Fe protein. This system should be useful in probing many aspects of the Fe protein catalytic function. Characterization of a heterodimeric Fe protein for which the Asp^{39} residue within only one of the two Fe protein subunits was substituted by Asn^{39} has led to the following conclusions. The contributions from each subunit to the nucleotide-induced conformational changes that affect the biophysical features of the [4Fe-4S] cluster are additive. The acceleration

of the rate of electron transfer from the Fe protein to the MoFe protein is the consquence of an additive effect resulting from the binding/hydrolysis of one MgATP to each Fe protein subunit. The formation of a tight Fe protein−MoFe protein complex can result from the modification of only one subunit of the Fe protein.

ACKNOWLEDGMENT

We thank Drs. Jason Christiansen and Jennifer Huyett for helpful discussions and Dr. Thomas Grover of the Biotechnology Group at Utah State University for assistance with the mass spectral analysis.

REFERENCES

1. Kim, J., and Rees, D. C. (1992) *Science 257*, 1677−1682.
2. Shah, V. K., and Brill, W. J. (1977) *Proc. Natl. Acad. Sci. U.S.A. 74*, 3249−3253.
3. Peters, J. W., Fisher, K., Newton, W. E., and Dean, D. R. (1995) *J. Biol. Chem. 270*, 27007−27013.
4. Chan, J. M., Christiansen, J., Dean, D. R., and Seefeldt, L. C. (1999) *Biochemistry 38*, 5779−5785.
5. Lowe, D. J., Fisher, K., and Thorneley, R. N. F. (1993) *Biochem. J. 292*, 93−98.
6. Ma, L., Brosius, M. A., and Burgess, B. K. (1996) *J. Biol. Chem. 271*, 10528−10532.
7. Georgiadis, M. M., Komiya, H., Chakrabarti, P., Woo, D., Kornuc, J. J., and Rees, D. C. (1992) *Science 257*, 1653−1659.
8. Seefeldt, L. C., and Dean, D. R. (1997) *Acc. Chem. Res. 30*, 260−266.
9. Burgess, B. K., and Lowe, D. J. (1996) *Chem. Rev. 96*, 2983−3011.
10. Hageman, R. V., and Burris, R. H. (1978) *Proc. Natl. Acad. Sci. U.S.A. 75*, 2699−2702.
11. Thorneley, R. N. F., and Lowe, D. J. (1984) *Biochem. J. 224*, 903−909.
12. Cordewener, J., Haaker, H., Van Ewijk, P., and Veeger, C. (1985) *Eur. J. Biochem. 148*, 499−508.
13. Chen, L., Gavini, N., Tsuruta, H., Eliezer, D., Burgess, B. K., Doniach, S., and Hodgson, K. O. (1994) *J. Biol. Chem. 269*, 3290−3294.
14. Zumft, W. G., Mortenson, L. E., and Palmer, G. (1974) *Eur. J. Biochem. 46*, 525−535.
15. Stephens, P. J., McKenna, C. E., Smith, B. E., Nguyen, H. T., McKenna, M. C., Thomson, A. J., Devlin, F., and Jones, J. B. (1979) *Proc. Natl. Acad. Sci. U.S.A. 76*, 2585−2589.
16. Wolle, D., Dean, D. R., and Howard, J. B. (1992) *Science 258*, 992−995.
17. Seefeldt, L. C., Morgan, T. V., Dean, D. R., and Mortenson, L. E. (1992) *J. Biol. Chem. 267*, 6680−6688.
18. Seefeldt, L. C., and Mortenson, L. E. (1993) *Protein Sci. 2*, 93−102.
19. Ryle, M. J., Lanzilotta, W. N., Mortenson, L. E., Watt, G. D., and Seefeldt, L. C. (1995) *J. Biol. Chem. 270*, 13112−13117.
20. Lanzilotta, W. N., Fisher, K., and Seefeldt, L. C. (1997) *J. Biol. Chem. 272*, 4157−4165.
21. Lanzilotta, W. N., Ryle, M. J., and Seefeldt, L. C. (1995) *Biochemistry 34*, 10713−10723.
22. Jacobson, M. R., Brigle, K. E., Bennett, L. T., Setterquist, R. A., Wilson, M. S., Cash, V. L., Beynon, J., Newton, W. E., and Dean, D. R. (1989) *J. Bacteriol. 171*, 1017−1027.
23. Burgess, B. K., Jacobs, D. B., and Stiefel, E. I. (1980) *Biochim. Biophys. Acta 614*, 196−209.
24. Christiansen, J., Goodwin, P. J., Lanzilotta, W. N., Seefeldt, L. C., and Dean, D. R. (1998) *Biochemistry 37*, 12611−12623.
25. Chromy, V., Fischer, J., and Kulhanek, V. (1974) *Clin. Chem. 20*, 1362−1363.
26. Anderson, G. L., and Howard, J. B. (1984) *Biochemistry 23*, 2118−2122.
27. Hathaway, G. M., Lundak, T. S., Tahara, S. M., and Traugh, J. A. (1979) *Methods Enzymol. 60*, 495−511.
28. Seefeldt, L. C., and Ensign, S. A. (1994) *Anal. Biochem. 221*, 379−386.
29. Ryle, M. J., and Seefeldt, L. C. (2000) *J. Biol. Chem. 275*, 6214−6219.
30. Weast, R. C. (1988) *CRC Handbook of Chemistry and Physics*, 69th ed.; CRC Press, Boca Raton, FL
31. Ryle, M. J., Lanzilotta, W. N., Seefeldt, L. C., Scarrow, R. C., and Jensen, G. M. (1996) *J. Biol. Chem. 271*, 1551−1557.
32. Ljones, T., and Burris, R. H. (1978) *Biochemistry 17*, 1866−1872
33. Lanzilotta, W. N., Fisher, K., and Seefeldt, L. C. (1996) *Biochemistry 35*, 7188−7196.
34. Orme-Johnson, W. H., Hamilton, W. D., Jones, T. L., Tso, M. Y. W., Burris, R. H., Shah, V. K., and Brill, W. J. (1972) *Proc. Natl. Acad. Sci. U.S.A. 69*, 3142−3145
35. Smith, B. E., Lowe, D. J., and Bray, R. C. (1973) *Biochem. J. 135*, 331−341.
36. Walker, G. A., and Mortenson, L. E. (1974) *Biochemistry 13*, 2382−2388.
37. Ryle, M. J., and Seefeldt, L. C. (1996) *Biochemistry 35*, 4766−4775.
38. Wolle, D., Kim, C., Dean, D., and Howard, J. B. (1992) *J. Biol. Chem. 267*, 3667−3673.
39. Seefeldt, L. C. (1994) *Protein Sci. 3*, 2073−2081.
40. Ryle, M. J., Lanzilotta, W. N., and Seefeldt, L. C. (1996) *Biochemistry 35*, 9424−9434.
41. Ryle, M. J., and Seefeldt, L. C. (1996) *Biochemistry 35* (49), 15654−15662.
42. Gavini, N., and Burgess, B. K. (1992) *J. Biol. Chem. 267*, 21179−21186.
43. Bursey, E. H., and Burgess, B. K. (1998) *J. Biol. Chem. 273* (45), 29678−29685.
44. Bursey, E. H., and Burgess, B. K. (1998) *J. Biol. Chem. 273* (27), 16927−16934.
45. Lanzilotta, W. N., Parker, V. D., and Seefeldt, L. C. (1999) *Biochim. Biophys. Acta 1429*, 411−421.
46. Thorneley, R. N. F., Ashby, G., Howarth, J. V., Millar, N. C., and Gutfreund, H. (1989) *Biochem. J.* 264, 657−661.
47. Schindelin, H., Kisker, C., Schlessman, J. L., Howard, J. B., and Rees, D. C. (1997) *Nature 387*, 370−376.
48. Kraulis, P. J. (1991) *J. Appl. Crystallogr. 24*, 946−950.
49. Merritt, E. A., and Murphy, M. E. P. (1994) *Acta Crystallogr. D50*, 869−873.

BI000219Q